ChemComm

COMMUNICATION

View Article Online
View Journal | View Issue

Cite this: *Chem. Commun.*, 2022, **58**, 5463

Received 5th March 2022,
Accepted 6th April 2022

DOI: 10.1039/d2cc01322c

rsc.li/chemcomm

UV degradation of poly(lactic acid) materials through copolymerisation with a sugar-derived cyclic xanthate†

Craig Hardy, [a] Gabriele Kociok-Köhn [b] and Antoine Buchard *[a]

The copolymerisation of L-Lactide with a cyclic xanthate monomer derived from tri-*O*-acetyl-D-glucal has been used to incorporate thionocarbonate and thioester linkages into a polyester backbone. The poly(lactide-*co*-xanthate) copolymers show enhanced UV-degradability compared to PLA, with 40% mass loss within 6 hours of UV exposure (365 nm) for only 3% of sulfur-containing linkages.

Amidst the environmental persistence and reliance on fossil-based resources of the most common polymers, polymers based on renewable resources, and which can be degraded, have been investigated as alternatives.[1–3] Poly(lactic acid) (PLA) is a thermoplastic aliphatic polyester derived from lactic acid and is perhaps the most widely studied degradable and renewable polymer. While PLA degrades under industrial composting conditions (62 ± 4 °C, >60% relative humidity) within weeks, it lacks facile degradability in natural environments, *e.g.* in soil or in seawater.[4,5] One strategy to adjust the degradation of PLA has been the copolymerisation of lactide (LA) with other monomers resulting in linkages more susceptible to hydrolysis.[4,6] Once oligomeric, PLA indeed dissolves quicker and is attacked by enzymes more effectively. Thus, in biomedical applications, poly(lactic-*co*-glycolic acid) (PLGA) is a common material.[7] PLA hydrolytic degradation has also been enhanced recently by copolymerisation with cyclic phosphoester[8] and salicylates.[9] However, to the best of our knowledge, no modification of PLA has been directed at enhancing its degradability towards stimuli other than hydrolysis, such as light.

As part of our wider research programme on renewable polymers, we, amongst others, have been investigating the incorporation of monosaccharide units into polymer backbones. The natural abundance, structural diversity and functionalisation potential of sugars make them a renewable resource with tremendous potential for sustainable materials.[10,11] Of relevance here, we have thus reported the ring-opening copolymerisation of a xylose-based oxetane with CS_2, which yield polythiocarbonates that rapidly degrade under UV radiation.[12] We also previously reported the Ring-Opening Polymerisation (ROP) of cyclic xanthates from C5 sugars (D-ribose and D-xylose).[13] However, their synthesis was challenging, with extensive purification needed for ROP. Herein, our hypothesis has been that the copolymerisation of lactide with a cyclic xanthate would allow the incorporation of UV-sensitive linkages into PLA. We report the synthesis of a novel cyclic xanthate monomer derived from D-glucal, its ring-opening polymerisation (ROP) and copolymerisation with L-lactide, which results in unprecedented UV-degradable poly(lactic acid).

To circumvent the difficulties met previously, we selected tri-*O*-acetyl-D-glucal as starting material, a commercial derivative of C6 sugar D-glucose, previously used for polycarbonate synthesis by ROP. One attractive feature of glucal-derived monomers is the incorporation in the polymer backbone of a cyclic alkene, primed for post-polymerisation modifications. Building on the strategy developed by Wooley and coworkers,[14] the synthesis of the desired cyclic xanthate involved four high-yielding synthetic steps (59% yield) from tri-*O*-acetyl-D-glucal: Ferrier rearrangement, deprotection under Zemplén conditions, tosylation at the C-6 position, then cyclisation using CS_2 (Scheme 1).

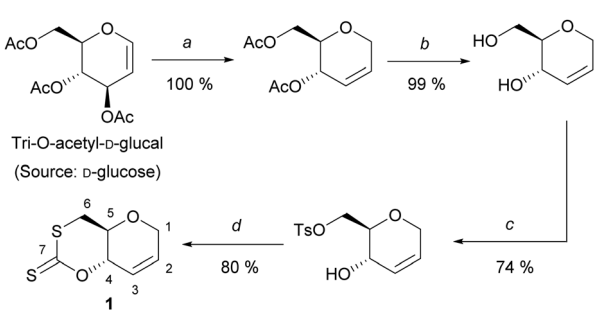

Scheme 1 Synthesis of **1**; (a) Et_3SiH, BF_3OEt_2, DCM, 0 °C, 3 h; (b) NaOMe, MeOH, rt, 2 h; (c) TsCl, Pyridine, rt, 20 h; (d) CS_2, *t*-BuOK, THF, 0 °C, 3 h.

[a] *Centre for Sustainable and Circular Technologies, Department of Chemistry, University of Bath, Bath, BA2 7AY, UK. E-mail: a.buchard@bath.ac.uk*
[b] *Materials and Chemical Characterisation Facility (MC²), University of Bath, UK*

† Electronic supplementary information (ESI) available: Experimental details; spectroscopic and crystallographic data for **1**; SEC traces, spectroscopic and thermal (TGA, DSC) data for the polymers. CCDC 2089243. For ESI and crystallographic data in CIF or other electronic format see DOI: https://doi.org/10.1039/d2cc01322c

After recrystallisation in ethanol, cyclic xanthate **1**, was isolated as pale-yellow crystals, and was characterized by multinuclear NMR and FT-IR spectroscopies. Unambiguously, $^{13}C\{^1H\}$ NMR analysis identified a signal at $\delta_C \approx 208$ ppm, characteristic of the C(S)SO linkage of cyclic xanthates.[15] Molecular structure and stereochemistry were further corroborated by single crystal X-ray diffraction crystallography (Fig. S23, ESI†).

The ROP of **1** was successfully conducted at room temperature (rt) in dichloromethane (DCM), using 1,5,7-triazabicyclo[4.4.0]dec-5-ene (TBD) as catalyst, 4-methylbenzyl alcohol (4-MeBnOH) as initiator (Table 1). Early trials with other organocatalysts indeed resulted in lower activities (ESI† Table S1). At 1 mol L^{-1} initial monomer concentration, ROP proceeded readily, rapidly reaching a plateau, with only marginal increase in monomer conversion when increasing reaction times from 6 h (71–72%; Table 1, entries 1–3) to 24 h (77–78%; Table 1, entries 4–6). This plateau in monomer conversion is indicative of an equilibrium limited opening of the ring and is consistent with the exceptional stability (towards air, moisture, and heat) of cyclic xanthate **1**. This is in stark contrast with the analogous 6-membered cyclic carbonates, for which the ROP equilibrium lies heavily towards the polymeric products (>99%),[14,16–18] highlighting how exchanging oxygen for sulfur atoms strongly impacts ring strain and polymerisability.

As expected from an equilibrium-limited ROP process, initial monomer concentration could be manipulated to reach higher monomer conversion, and 90% conversion was achieved for $[\mathbf{1}]_0 = 2.0$ mol L^{-1} (Table 1, entry 8). Interestingly for polymer chemical recyclability, a near quantitative recovery of the monomer is observed when poly(**1**) is stirred in the presence of TBD in dilute conditions (0.1 mol L^{-1}). The temperature dependence of the ROP equilibrium was also investigated in 1,2-dichloroethane (DCE) at fixed initial monomer concentration, catalyst and initiator loadings. Decreasing temperature from 60 °C to 0 °C resulted in an increase in monomer conversion from 2% up to 85%. Below 0 °C **1** was no longer soluble resulting in no reaction. A plot of $\ln([\mathbf{1}]_{eq})$ *vs.* $1/T$ gave an approximation of the polymerisation thermodynamic parameters (Fig. S46, ESI†): $\Delta H_p = -25.6$ kJ mol^{-1} and $\Delta S_p = -80$ J mol^{-1}. A similar study using THF instead of DCE also gave an estimation of these parameters in THF (Fig. S47, ESI†; $\Delta H_p = -22.0$ kJ mol^{-1} and $\Delta S_p = -61$ J mol^{-1} K^{-1}; revealing a moderate increase in the enthalpy of polymerisation, but with little impact on polymerisability.

Upon reaction completion, the polymer products could be isolated by precipitation in diethyl ether, and SEC was utilised to estimate number-average molar masses (M_n) and dispersities ($Đ_M$). Discrepancy between expected molar masses and those calculated by SEC was found (Table 1), in addition to limitations in obtaining high molar mass polymers, which both may be due to impurities in the monomer acting as chain-transfer agents. Nevertheless, polymers of up to 10 700 g mol^{-1} ($Đ_M$ 1.76) could be obtained, some control of the polymerisation was indicated by the linear relationship between monomer conversion and M_n (Fig. S45, ESI†) and first-order kinetics with respect to monomer concentration (Fig. S40–S44, ESI†).

$^{13}C\{^1H\}$ NMR spectroscopy was primarily used to investigate the microstructure of poly(**1**) (Fig. 1). Two major thiocarbonyl resonances at $\delta_C \approx 194$ and 223 ppm, of similar intensity, could be seen and were assigned to a mono-thionocarbonate ($C(S)O_2$) environment and a tri-thiocarbonate environment ($C(S)S_2$), respectively.[12,13] Only a small amount of xanthate linkages (SC(S)O; 1–2%) could be identified from a minor resonance at $\delta_C \approx 214$ ppm.[19] ^1H NMR spectra also featured a CH–O ($\delta_H = 5.68$–5.75) and a shielded CH_2–S ($\delta_H = 3.68$–3.58) proton environments (Fig. S24, ESI†). Collectively, this data suggests the ROP of **1** proceeds *via* the alternating opening of **1**

Table 1 Ring-opening polymerisation of **1** catalysed by TBD[a]

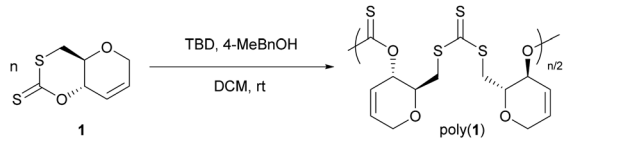

Entry	$[\mathbf{1}]_0:[TBD]_0:[I]_0$[b]	Time (h)	Conv (%)[c]	$M_{n,calc}$[d]	$M_{n,NMR}$[e]	$M_{n,SEC}$ [$Đ_M$][f]
1	100 : 1 : 1	6	71	13.5	9.2	6.8 [1.73]
2	50 : 1 : 1	6	71	6.8	5.5	5.2 [1.58]
3	25 : 1 : 1	6	72	3.5	2.8	4.0 [1.44]
4	100 : 1 : 1	24	77	14.6	10.1	8.7 [1.75]
5	50 : 1 : 1	24	77	7.4	5.6	5.9 [1.69]
6	25 : 1 : 1	24	78	3.8	2.8	4.7 [1.51]
7[g]	100 : 1 : 1	24	58	9.7	5.9	4.3 [1.58]
8[h]	100 : 1 : 1	24	90	17.4	8.1	10.0 [1.68]
9	150 : 1 : 1	24	69	19.6	13.6	10.5 [1.68]
10	200 : 1 : 1	24	75	28.4	15.9	10.7 [1.76]

[a] Polymerisations were carried out at rt, under an argon atmosphere, in anhydrous CH_2Cl_2 solvent with initial $[\mathbf{1}]_0 = 1$ mol L^{-1} (**1** = monomer), unless stated otherwise. [b] I = 4-methylbenzylalcohol. [c] Monomer conversion to polymer, calculated based on the relative integration of the H-4′ proton signal of **1** ($\delta_H = 4.79$ ppm) and poly(**1**) ($\delta_H = 5.75$–5.68 ppm), in the ^1H NMR spectrum. [d] Number-average molar mass as calculated using $M_r(I) + (M_r(monomer) \times [monomer]_0/[I]_0 \times conv/100\%)$ (kg mol^{-1}). [e] Number-average molar mass calculated by the relative integration of the aromatic protons in I (δ = 7.30–7.15 ppm, 4 H) and H-4′ in poly(**1**) (kg mol^{-1}). [f] Number-average molar mass and Dispersity ($M_{n,SEC}$, $Đ_M$), calculated by SEC relative to polystyrene standards in THF eluent (kg mol^{-1}). [g] $[\mathbf{1}]_0 = 0.5$ mol L^{-1}. [h] $[\mathbf{1}]_0 = 2$ mol L^{-1}.

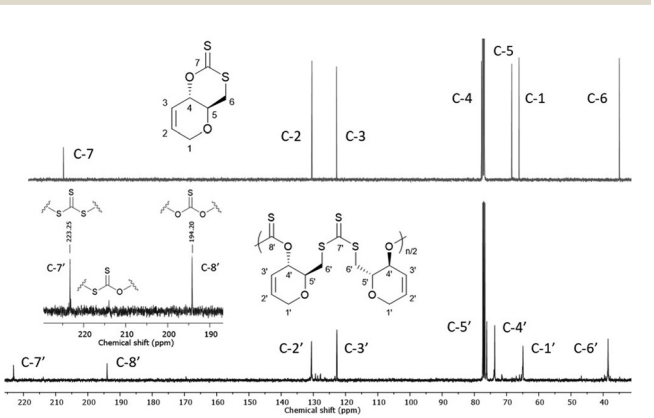

Fig. 1 $^{13}C\{^1H\}$ NMR spectra ($CDCl_3$) of **1** (top) and poly(**1**) (bottom) (Table 1, entry 4). (inset) Alternating $C(S)S_2$ and $C(S)O_2$ linkages observed for poly(**1**).

on either side of the xanthate thiocarbonyl, and subsequent selective chain propagation, yielding regioregular polymers with alternating C(S)S_2 and C(S)O_2 linkages, similar to what we observed for a xylose-based cyclic xanthate.

While MALDI-ToF mass spectrometry proved unsuccessful to probe further the macromolecular structure of poly(**1**), a good agreement between $M_{n,NMR}$ (estimated by end-group analysis) and $M_{n,SEC}$ values suggested the absence of major cyclic polymer species. When the ROP of **1** was carried out above 50 °C, especially in THF, a vibration at 1709 cm^{-1} in the FTIR spectra, characteristic of a carbon–oxygen double bond (C=O) vibrational mode (Fig. S52, ESI†), emerged. Two new carbonyl resonances could also be observed by $^{13}C\{^1H\}$ NMR spectroscopy, at 169 and 154 ppm, assigned to mono-thiocarbonate (C(O)SO) and carbonate (C(O)O_2) environments, respectively (Fig. S48, ESI†). This was indicative of some S–O exchange reactions, which *in situ* IR spectroscopy showed to occur after maximum monomer conversion is reached.

Poly(**1**)s were shown to be amorphous by differential scanning calorimetry (DSC) with a glass transition temperature (T_g) of 65 °C (Fig. S33–S36, ESI†; polymers of M_n 10 700 g mol^{-1} ($Đ_M$ 1.8) and 6800 g mol^{-1} ($Đ_M$ 1.6)). Thermogravimetric analysis (TGA) revealed the onset of thermal degradation ($T_{d5\%}$) to occur around 188 °C, with a final residual char of 19 and 15%, respectively (Figs. S37 and S38, ESI†).

Copolymerisation of **1** with L-lactide (L-LA) was first investigated through sequential monomer addition. 25 equivalents of **1** were first polymerised (DCM, rt; $[\mathbf{1}]_0:[TBD]_0:[MeBnOH]_0$ = 25 : 1 : 1; $[\mathbf{1}]_0$ = 1.0 mol L^{-1}). Then, after 6 hours and 78% conversion of **1** (M_n 4400 g mol^{-1}), 50 equivalents of L-LA were added to the reaction alongside some additional TBD (1.0 equiv.). After 2 hours, ^1H NMR spectroscopy showed 81 and 98% conversion of **1** and L-LA, respectively. After isolation of the polymer by precipitation, NMR spectroscopy confirmed the formation of a diblock copolymer (Fig. S57–S62, ESI†), while demonstrating the livingness of the ROP process (poly(**1**-*b*-LLA), M_n 17 300 g mol^{-1}; Fig. S63, ESI†).

One-pot copolymerisation of **1** with L-LA was also performed (Table 2). L-LA was quantitatively converted while as before, **1** reached a conversion plateau between 71–78%. ^1H and DOSY NMR analysis revealed the formation of a copolymer and its composition, which diverged from the monomers feed ratio as the proportion of **1** increased. In the carbonyl region of the $^{13}C\{^1H\}$ NMR spectra, alongside a major PLA ester signal at $\delta_C \approx 169$ ppm, all copolymers exhibited multiple thiocarbonyl resonances at $\delta_C \approx 194$ ppm, consistent with thionocarbonate (C(S)O_2) and thioester (C(O)S) environments (Fig. 2). As no xanthate or trithiocarbonate signals were observed, the probability of consecutively opening two or more molecules of **1** was deemed low. We propose that the incorporation of **1** in the copolymer mainly proceeds *via* the attack of **1** by a growing PLA chain and the cleavage of its C–S bond, producing a primary thiol which next opens a LA molecule. Copolymers with consecutive thionocarbonate and thioester linkages inserted within a polyester backbone are thus formed (poly(**1**-*co*-LLA)).

Even with as little as 1% **1** content, all poly(**1**-*co*-LLA)s were shown to be amorphous by DSC analysis (Table 2; Fig. S72–S76, ESI†), with T_gs ranging, with no identifiable trend, from 47 to 51 °C. TGA also revealed no obvious trend between the compositions of poly(**1**-*co*-LLA)s and their thermal stability, with $T_{d5\%}$ between 187 and 228 °C (Table 2; Fig. S77–S81, ESI†).

Building upon previous studies surrounding photodegradation,[20,21] as well as our experience with similar poly(thiocarbonates), poly(**1**) could be readily degraded under UV radiation (λ = 365 nm) in THF, with or without tris-(trimethylsilyl)-silane (TTMSS) to accelerate the reaction (Fig. S85 and S86, ESI†).[12,22] Analysis of the degradation products by ^1H NMR

Table 2 Ring-opening copolymerisation of **1** with L-LA catalysed by TBD[a]

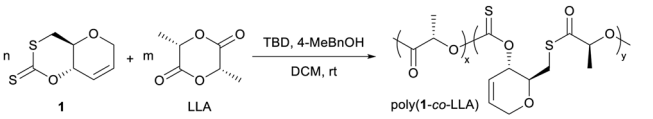

Entry	f_1/f_{LLA}	Conv. **1** (%) [b]	Conv. LLA (%)[c]	$M_{n,SEC}$ [$Đ_M$] [d]	F_1/F_{LLA} [e]	T_g (°C)[f]	$T_{d5\%}$ (°C)
1	2/98	71	98	22.5 [1.59]	1/99	51	228
2	5/95	71	99	13.2 [1.66]	3/97	51	222
3	10/90	71	99	14.8 [1.70]	6/94	49	223
4	20/80	77	98	15.8 [1.80]	16/84	47	187
5	50/50	71	98	25.1 [1.86]	29/71	50	200

[a] Polymerisations were carried out at rt, for 20 h, under an argon atmosphere, in anhydrous CH_2Cl_2 solvent with initial $[\mathbf{M}_t]_0$ = 1 mol L^{-1} ($\mathbf{M}_t$ = **1** + L-LA) and $[\mathbf{M}_t]_0:[TBD]_0:[4\text{-MeBnOH}]_0$ = 100 : 1 : 1. [b] Monomer conversion to polymer, calculated based on the relative integration of the H-4′ proton signal of **1** (δ_H = 4.79 ppm) and poly(**1**) (δ_H = 5.75–5.68 ppm), in the ^1H NMR spectrum. [c] Monomer conversion to polymer, calculated based on the relative integration of the lactide alkoxy proton signals in the crude ^1H NMR spectrum. [d] Number-average molecular weight and Dispersity ($M_{n,SEC}$, $Đ_M$), calculated by SEC relative to polystyrene standards in THF eluent (kg mol^{-1}). [e] Copolymer compositions determined by integration of the ^1H NMR spectra of the purified copolymers. [f] Values taken from DSC second heating cycle.

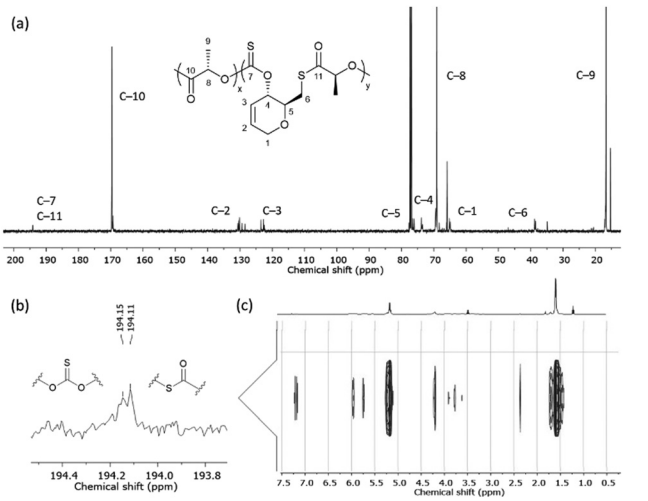

Fig. 2 (a) $^{13}C\{^1H\}$ NMR spectrum ($CDCl_3$) with (b) C(S)O_2 and C(O)S linkages observed for poly(**1**-*co*-LLA), and (c) ^1H DOSY NMR spectrum ($CDCl_3$) of isolated poly(**1**-*co*-LLA) (Table 2, entry 4).

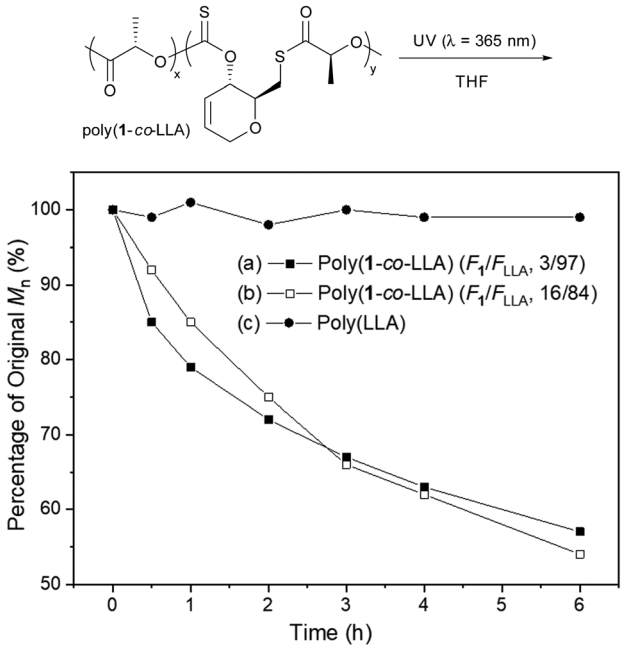

Fig. 3 Percentage of original M_n *vs.* time, following the exposition of poly(**1**-*co*-LLA) copolymers to UV irradiation (λ = 365 nm). The reactions were performed at rt with $[\text{poly}(\mathbf{1}\text{-}co\text{-LLA})]_0$ = 0.040 mol L^{-1}. (a) Poly(**1**-*co*-LLA) (F_1/F_{LLA}, 3/93) ($M_{n,SEC}$ = 13,200 g mol^{-1}, $Đ_M$ = 1.66), (b) poly(**1**-*co*-LLA) (F_1/F_{LLA}, 16/84) ($M_{n,SEC}$ = 15,800 g mol^{-1}, $Đ_M$ = 1.80) and (c) poly(LLA) ($M_{n,SEC}$ = 12,800 g mol^{-1}, $Đ_M$ = 1.12).

spectroscopy proved difficult, although the absence of the H-6' proton signals suggested the complete breakdown of the trithiocarbonate linkages.

The degradation of statistical copolymers poly(**1**-*co*-LLA)s under UV irradiation in THF, in the absence of TTMSS, was also investigated (Fig. 3, polymers from entries 2 and 4, Table 2). Satisfyingly, a gradual decrease in molar mass was observed, which correlated well with the quantity of thionocarbonate/thioester linkages in the polymer. Analysis of the degradation products by ^{1}H NMR spectroscopy revealed a breakdown of the thionocarbonate/thioester linkages leaving predominantly PLLA species (Fig. S87 and S88, ESI†). Under identical conditions, no change was observed for PLLA, supporting the hypothesis that degradation is due to sulfur-containing linkages. UV-Vis spectra of the polymers (Fig. S82 and S83, ESI†) displayed a singular absorbance within the ultraviolet region ($\lambda_{max} \approx 306$ nm) confirming that UV irradiation is the stimulus promoting photodegradation. Photodegradation of PLA has been relatively unexplored, and often requires the incorporation of light responsive nanoparticles or the use of a nucleation agent, as well as extended periods of time (days/weeks) to reach significant levels of molar mass reduction (>20%).[23–25] Here, over 40% mass loss within 6 hours of UV exposure was seen, including for copolymers with as little as 3% thionocarbonate/thioester linkages.

In summary, we have synthesised a novel, bio-derived, unsaturated xanthate cyclic monomer, reported its ring-opening polymerisation and characterised the resulting poly(thiocarbonate)s. The sugar-based monomer was also copolymerised with L-lactide towards block and statistical copolymers. Even at low content, introducing UV-cleavable sulfur-containing linkages into PLA enabled its effective photodegradation into biodegradable oligomeric species. The mechanism of degradation requires to be investigated in detail, and this strategy remains to be translated to real-life plastics objects, but it has the potential to increase the environmental degradability of PLA without significantly affecting its material properties.

We thank the Royal Society (UF\160021, fellowship to AB; RGF\EA\201023; RGF\EA\180028, studentship to CH) for research funding.

Conflicts of interest

There are no conflicts of interest to declare.

Notes and references

1 R. Geyer, J. R. Jambeck and K. L. Law, *Sci. Adv.*, 2017, **3**, e1700782.
2 J.-G. Rosenboom, R. Langer and G. Traverso, *Nat. Rev. Mater.*, 2022, **7**, 117–137.
3 S. Walker and R. Rothman, *J. Cleaner Prod.*, 2020, **261**, 121158.
4 P. McKeown and M. D. Jones, *Sustainable Chem.*, 2020, **1**, 1–22.
5 S. M. Emadian, T. T. Onay and B. Demirel, *Waste Manage.*, 2017, **59**, 526–536.
6 N. F. Zaaba and M. Jaafar, *Polym. Eng. Sci.*, 2020, **60**, 2061–2075.
7 H. K. Makadia and S. J. Siegel, *Polymers*, 2011, **3**, 1377–1397.
8 T. Rheinberger, J. Wolfs, A. Paneth, H. P.Paneth and F. R. Wurm, *J. Am. Chem. Soc.*, 2021, **143**, 15784–15790.
9 H. J. Kim, M. Hillmyer and C. Ellison, *J. Am. Chem. Soc.*, 2021, **143**, 15784–15790.
10 G. L. Gregory, E. M. López-Vidal and A. Buchard, *Chem. Commun.*, 2017, **53**, 2198–2217.
11 S. L. Kristufek, K. T. Wacker, Y.-Y. T. Tsao, L. Su and K. L. Wooley, *Nat. Prod. Rep.*, 2017, **34**, 433–459.
12 T. M. McGuire and A. Buchard, *Polym. Chem.*, 2021, **12**, 4253–4261.
13 E. M. López-Vidal, G. L. Gregory, G. Kociok-Köhn and A. Buchard, *Polym. Chem.*, 2018, **9**, 1577–1582.
14 A. T. Lonnecker, Y. H. Lim and K. L. Wooley, *ACS Macro Lett.*, 2017, **6**, 748–753.
15 M. Luo, X.-H. Zhang and D. J. Darensbourg, *Macromolecules*, 2015, **48**, 5526–5532.
16 K. Mikami, A. T. Lonnecker, T. P. Gustafson, N. F. Zinnel, P.-J. Pai, D. H. Russell and K. L. Wooley, *J. Am. Chem. Soc.*, 2013, **135**, 6826–6829.
17 Y. Song, X. Ji, M. Dong, R. Li, Y.-N. Lin, H. Wang and K. L. Wooley, *J. Am. Chem. Soc.*, 2018, **140**, 16053–16057.
18 Y. Song, X. Yang, Y. Shen, M. Dong, Y.-N. Lin, M. B. Hall and K. L. Wooley, *J. Am. Chem. Soc.*, 2020, **142**, 16974–16981.
19 D. J. Darensbourg, J. R. Andreatta, M. J. Jungman and J. H. Reibenspies, *Dalton Trans.*, 2009, 8891–8899.
20 T. Sakamoto, K. Watanabe, Y. Shichibu, K. Konishi, S.-I. Sato and T. Nakano, *J. Poly. Sci. Poly. Chem.*, 2011, **49**, 945–956.
21 M. Suzuki, A. Watanabe, R. Kawai, R. Sato, S.-I. Matsuoka and S. Kawauchi, *Polymer*, 2021, **215**, 123386.
22 B. A. Fultz, D. Beery, B. M. Coia, K. Hanson and J. G. Kennemur, *Polym. Chem.*, 2020, **11**, 5962–5968.
23 W. Han, C. Luo, Y. Yang, J. Ren, H. Xuan and L. Ge, *Colloids Surf., A*, 2018, **558**, 488–494.
24 M. Tu-morn, N. Pairoh, W. Sutapun and T. Trongsatitkul, *Mater. Today: Proc*, 2019, **17**, 2048–2061.
25 J. Salač, J. Šerá, M. Jurča, V. Verney, A. A. Marek and M. Koutný, *Materials*, 2019, **12**, 481.

